III. Spacecraft Power

GUIDANCE AND CONTROL DIVISION

A. Solar Power System Definition Studies,

W. R. Yeaney

1. Introduction

The overall objective of this effort is to investigate the problems associated with developing spacecraft power systems for unmanned planetary missions. The effort stresses development of the technology required to solve system design problems associated with meeting JPL mission requirements. One task which has been undertaken is the investigation and development of computer programs for power system design and analysis.

2. Present Activities

The investigation of computer programs available for the spacecraft solar power system analysis and design was approached in a three phase program. The first and continuing phase is to develop in-house capability to meet the immediate program needs.

a. JPL-developed computer programs. A computer program has been developed to show in a parametric manner the interaction of the power profile, the power source size and weight, and the orbit characteristics in a Mars-orbiting *Voyager*-class spacecraft. A series of computer plotting programs demonstrate the possibility of a preliminary power source analysis, given a representative power profile and mission constraints. The programs accommodate most of the missions requirements, e.g., planetary orbiter, planetary fly-by, and planetary lander. The computations have been made using energy balance equations which consider: (1) battery capacity, energy density, discharge depth, and charge efficiency, (2) solar array area, overcapacity, and energy density, (3) orbit time and eclipse duration, and (4) load profile variations. Computer plots give comparisons of the various parameters in order to make system optimization possible

An additional computer program has been developed for reflecting arbitrary load profiles back to the power sources. This program keeps an inventory of the various power requirements for the science and engineering experiments included in a *Mariner*-class spacecraft. As these loads vary with mission function, the total user load profile is calculated. The user load profile is then reflected back through the conversion equipment, accounting for various device efficiencies, and the effect on the power source is calculated.

Further in-house programs are being developed to predict array electrical characteristics. The programs calculate panel short-circuit current, open-circuit voltage,

maximum power and temperature with variation of the solar cell type, the number of cells in series and parallel, the panel absorptivity and emissivity, and the solar intensity.

b. Search for power system analysis programs. During the second phase, a JPL literature search compiled information on the sources of computerized power system analysis programs and techniques. The information from this literature search provided the basis for a NASA center and industry survey (phase three).

c. Integration of other programs into JPL computer system. During phase th , discussions have been held with NASA Mission A Division (Moffet Field), Goddard, Manned Spacecraft Center, Ames, Langley, and the Electronic Research Center in order to obtain a better understanding of their present and planned efforts. In addition, the major aerospace companies have been surveyed to obtain information on additional computer programs. From the survey, several computer programs have been obtained and integrated into the JPL computer system. The first computer program simulates the solar array voltage and current relation for a given intensity and temperature. The second computer program is a thermal model for determining the solar array temperature as a function of solar intensity and panel absorptivity and emissivity properties. The third program sizes a complete satellite electrical system consisting of solar panels, battery, converter, and inverter from existing empirical data. In this program, the system requirements are:

(1) Solar array weight, area, and series and parallel connections.

(2) Battery weight, volume, capacity, and cell number.

(3) Conversion efficiency and energy density.

(4) Temperature profile.

(5) Load profile.

With these selections, the program will be used to "fly" the various missions and check energy balance, solar array design, reliability and redundancy provisions, and thermal control requirements.

3. Future Activities

In the future, additional computer programs will be investigated for adaptation or modification to meet JPL/NASA requirements. The in-house computer program effort will also be continued.

B. Shielding Analysis for Radioisotope Power Systems, *P Gingo*

A portion of the activities being pursued under the Nuclear Power System Definition Studies involves the evaluation of the shielding problems associated with the use of a radioisotope thermoelectric generator (RTG) in a spacecraft power system. Early in this program it became evident that the development of a computer capability for the analysis of this problem would be required because of the complexity of the problem. These computer programs will calculate the neutron and gamma fluxes generated by the radioisotope which will serve as a model for the experimental tests to completely specify the radioisotope radiation spectrum. Three tasks were undertaken to achieve this capability.

1. Available Computation Methods

The first task undertaken was a review of available nuclear computer codes. Among the sources investigated for nuclear codes were the libraries of the Radiation Shielding Information Center (RSIC), Los Alamos Scientific Laboratory, Livermore Radiation Laboratory, Martin Company, Atomics International and the Valley Forge Division of the General Electric Company. After this initial review, it became evident that the required nuclear codes should include the following three methods of calculation:

a. The Kernel integration method. This rapidly convergent program requires a very low execution time. The inherent difficulty with this method is that it is essentially a ray tracing technique which will not account for multiple scattering and geometry effects. The accuracy of these calculations is limited to the accuracy of the buildup factors and the cross sections used.

b. The Boltzmann transport equation. This requires more execution time than the Kernel integration method but is considerably more accurate. Geometry effects are limited to the sphere, slab and the cylinder.

c. Monte Carlo scattering. Execution time is 0.5 hr or more and is very sensitive to the starting constants used. This method includes multiple scattering and is currently the most accurate method used. Because execution time is very long, the Monte Carlo scattering method is generally used once the RTG design is fixed.

In addition to the nuclear computing codes, neutron and gamma cross sections had to be obtained which would be consistent with each nuclear code and its method of calculation.

The work to date has been to collect and integrate the nuclear codes with the necessary cross sections to utilize these nuclear codes. The following has been accomplished to achieve this RTG analysis capability.

2. Introduction of Nuclear Computing Codes to JPL

The Los Alamos DTF-IV Neutron Transport Code was received by the JPL Computation Center directly from Los Alamos and also from the Martin Company. The version given by the Martin Company is a 3-link overlay which would fit into the JPL 7094 Direct Couple Operating System (DCOS) Storage. To date, numerous changes have been made to the Martin version of the DTF-IV Transport Code. These changes include:

(1) Resizing of "COMMON" to fit the program into our 32-K machine.

(2) Going to alternate input and output modes in order to gain more available storage for the COMMON arrays.

(3) Extension of dosage calculations from spherical to cylindrical and slab geometries.

(4) Correction of specific linearizing indexing conventions to permit the inclusion of higher order terms into the transport equation, which was of the zeroth order in the Martin Baltimore version of the code (simple diffusion equation), thus greatly extending the potential accuracy available to the user.

(5) Running various check problems from straight card input. The DTF IV program is now fully operational in this respect.

The "QUAD" Kernel Integration Code available from the Los Alamos Scientific Laboratory was also received and integrated into the JPL DCOS 7094.

The current difficulty with this program is the problem of specifying the correct buildup factors which essentially are for single element media. To avoid this, buildup factors can be used which correspond to a mixture of elements taken from the General Electric 14-0 Nuclear Codes program.

The GE 14-0 Code is also a Kernel integration program which allows for buildup factors directly due to a mixture of elements and is not necessarily averaged to correspond to one element as required by the "QUAD" program. The GE 14-0 program is available on tape at JPL but has not been made operational as yet.

No Monte Carlo Scattering programs have been requested since these represent a future requirement. A literature search will continue for rapidly convergent Monte Carlo programs.

The "MESNE" program was received from the Livermore Radiation Laboratory. This program will accept any basic neutron cross section library tape and convert this into flux averaged neutron cross sections for any specified group structure (limit is 20 groups). The flux averaged neutron cross sections would be the total cross sections, fission cross sections and the neutron transfer matrices which account for the neutron up-and-down scattering.

The "MESNE" program, originally written in Fortran II, has been subjected to a "SIFT" routine to eliminate any JPL 7094 DCOS inconsistencies. The program has been simultaneously converted to Fortran IV. At present, several subroutines are missing and have been requested from Dr. Howerton of the Livermore Radiation Laboratory. These subroutines, "ONMON," "OFFMON," and "DECODE," are used to generate the source tape and interrupt the program execution.

3. Introduction of Nuclear Cross Section Libraries to JPL

Neutron and gamma cross sections have been received to use with the nuclear codes presently operating at JPL. These basic cross sections presently available are the following:

(1) Effective Broad Beam Neutron Removal Cross Sections, reference AECD 3978, 1955.

(2) Gamma Ray Absorption Coefficients for elements and mixtures, reference XDC-59-10-19.

(3) 16-Group Hanson-Roach Neutron Cross Sections, reference GEMP-283.

(4) The complete Carroll Mills Los Alamos 18, 24, and 25 group neutron cross sections which include down-scattering matrices. Several isotopes, among them Pu 238 and Pu 241, are not included in this library.

(5) The Howerton evaluated neutron cross section library. This is the most current and complete library available. The "MESNE" program will be

used to reduce the Howerton evaluated library into any convenient neutron group structure (to an upper limit of 20 groups) which may be required for the RTG studies.

4. Calculations

A mockup of the modified RTG Headlight configuration generated by the General Electric Company as part of the *Voyager* follow-on work has been submitted for analysis into the DTF IV computer program utilizing the standard Hanson-Roach neutron 16 group. The gamma dose rates have been calculated at 28 detector points by the "QUAD" program with buildup factors taken from mixtures normally used in the GE 14-0 nuclear code. These calculations are used principally to further check the nuclear codes and will be resubmitted with more accurate assumptions, such as including silicon and the correct isotope specification of Haynes 25.

The RTG reentry vehicle configuration used in the present analysis is shown in Fig. 1. (See Sect. "A-A" of attached drawing.) This vehicle has been mocked-up for the neutron and gamma radiation analyses in the form depicted in Fig. 2. The calculations considered the modified RTG as a cylinder in the radial direction and a slab in the axial direction. The results of these calculations are given in Tables 1 and 2.

Table 1. Radioisotope thermal generator, total gamma dose rate versus time of exposure

Detector point coordinates, (R cm, 0 deg, Z cm)	Total dose rate, (Mrem/thermal-watt-hr)	
	After 1 day	After 5 years
1. (0, 0, 0)	4.1638×10^{-2}	13.30084×10^{-2}
2. (5, 0, 0)	3.2413×10^{-2}	10.6310×10^{-2}
3. (10, 0, 0)	1.5521×10^{-2}	5.8136×10^{-2}
4. (15, 0, 0)	1.0913×10^{-2}	4.3400×10^{-2}
5. (20, 0, 0)	8.8339×10^{-3}	3.4873×10^{-2}
6. (25, 0, 0)	7.3049×10^{-3}	2.8225×10^{-2}
7. (30, 0, 0)	6.1535×10^{-3}	2.3226×10^{-2}
8. (35, 0, 0)	5.1769×10^{-3}	1.9281×10^{-2}
9. (40, 0, 0)	4.3609×10^{-3}	1.6068×10^{-2}
10. (45, 0, 0)	3.7061×10^{-3}	1.3541×10^{-2}
11. (50.8, 0, 0)	3.10003×10^{-3}	1.1246×10^{-2}
12. (50.8, 0, 5)	3.4743×10^{-3}	1.2441×10^{-2}
13. (50.8, 0, 10)	3.7869×10^{-3}	1.3448×10^{-2}
14. (50.8, 0, 15.0)	3.9938×10^{-3}	1.4110×10^{-2}
15. (50.8, 0, 20)	4.0675×10^{-3}	1.4346×10^{-2}
16. (50.8, 0, 25)	3.9978×10^{-3}	1.4123×10^{-2}
17. (50.8, 0, 30)	3.7943×10^{-3}	1.3471×10^{-2}
18. (50.8, 0, 34.54)	3.5162×10^{-3}	1.2576×10^{-2}
19. (45, 0, 34.54)	4.3222×10^{-3}	1.5508×10^{-2}
20. (40, 0, 34.54)	5.2365×10^{-3}	1.8865×10^{-2}
21. (35, 0, 34.54)	6.4515×10^{-3}	2.3306×10^{-2}
22. (30, 0, 34.54)	8.0054×10^{-3}	2.9269×10^{-2}
23. (25, 0, 34.54)	1.0077×10^{-2}	3.7375×10^{-2}
24. (20, 0, 34.54)	1.2818×10^{-2}	4.8603×10^{-2}
25. (15, 0, 34.54)	1.6708×10^{-2}	6.5082×10^{-2}
26. (10, 0, 34.54)	2.2729×10^{-2}	9.2944×10^{-2}
27. (5, 0, 34.54)	6.1841×10^{-2}	22.024×10^{-2}
28. (0, 0, 34.54)	1.0376×10^{-1}	35.4671×10^{-2}

Table 2. Radioisotope neutron flux spectrum[a] (subcritical, $K = 0.96$)

Neutron energy group	Neutron energy (E_L)	Neutron current fraction detector coordinates		
		(R, θ, Z) (10.54 cm, 0, 10 cm)	(R, θ, Z) (0, 0, 34.54 cm)	(R, θ, Z) (0, 0, 0)
1	3.0 Mev	1.196×10^{-1}	1.218×10^{-1}	1.31×10^{-1}
2	1.4 Mev	2.67×10^{-1}	2.59×10^{-1}	2.62×10^{-1}
3	0.9 Mev	1.33×10^{-1}	1.33×10^{-1}	1.32×10^{-1}
4	0.4 Mev	1.96×10^{-1}	2.00×10^{-1}	2.00×10^{-1}
5	0.1 Mev	1.825×10^{-1}	1.895×10^{-1}	1.82×10^{-1}
6	17 kev	7.23×10^{-2}	7.2×10^{-2}	7.1×10^{-2}
7	3 kev	2.21×10^{-2}	1.94×10^{-2}	1.75×10^{-2}
8	0.55 kev	6.21×10^{-3}	4.34×10^{-3}	3.62×10^{-3}
9	0.1 kev	1.465×10^{-3}	6.89×10^{-4}	4.79×10^{-4}
10	30 ev	3.39×10^{-4}	1.12×10^{-4}	6.67×10^{-5}
11	10 ev	1.008×10^{-4}	2.36×10^{-5}	1.19×10^{-5}
12	3 ev	3.59×10^{-5}	5.77×10^{-6}	2.46×10^{-6}
13	1 ev	1.089×10^{-5}	1.24×10^{-6}	4.58×10^{-7}
14	0.4 ev	3.4×10^{-6}	2.76×10^{-7}	8.93×10^{-8}
15	0.1 ev	1.44×10^{-6}	7.97×10^{-8}	2.23×10^{-8}
16	thermal	5.37×10^{-7}	1.79×10^{-8}	4.20×10^{-9}

[a]Total neutron flux = neutron generated at detector times the neutron current fraction.

[b]The fuel density 10.7 gm/cm³ does not account for fuel void.

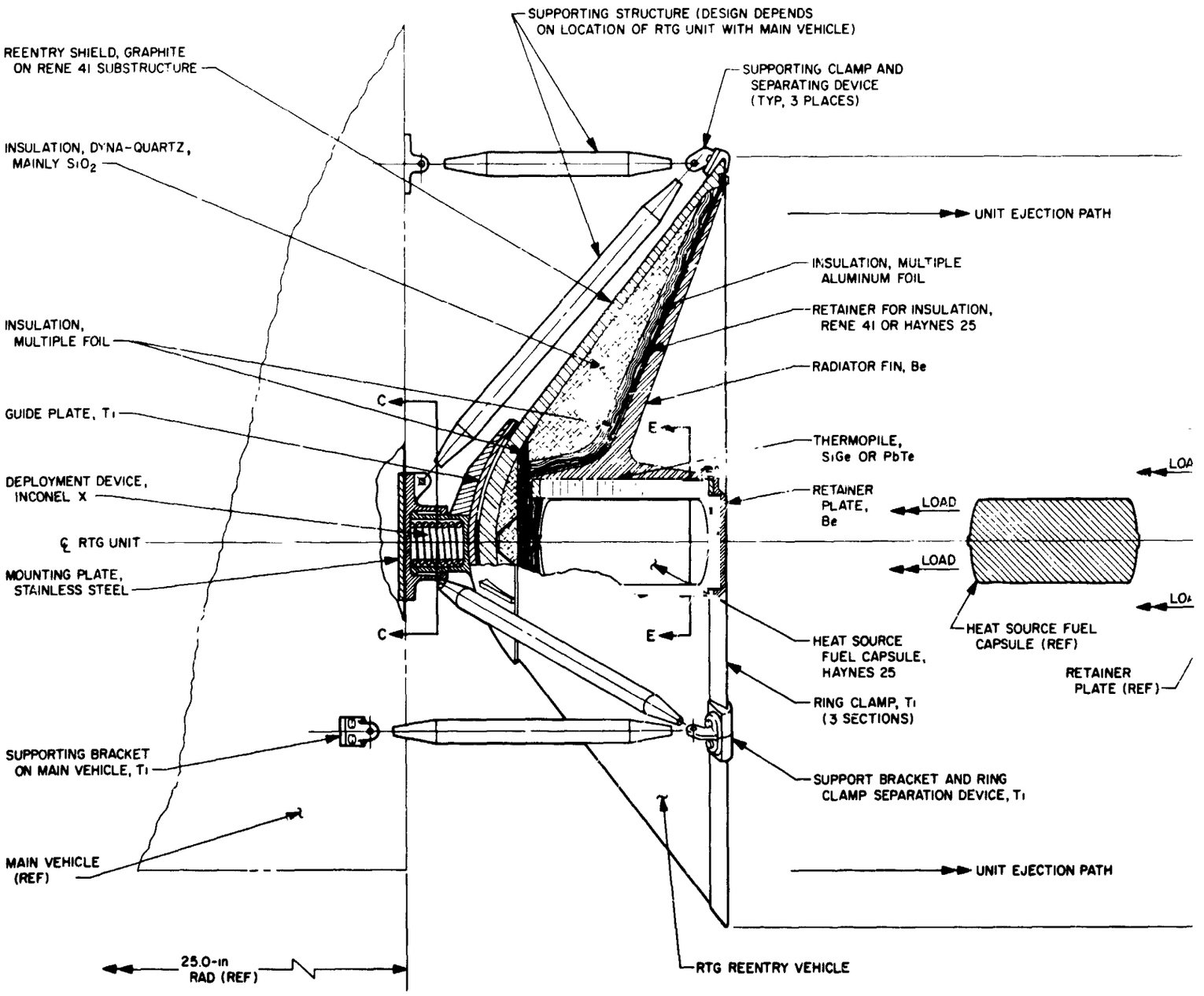
SUPPORTING STRUCTURE (DESIGN DEPENDS ON LOCATION OF RTG UNIT WITH MAIN VEHICLE)
REENTRY SHIELD, GRAPHITE ON RENE 41 SUBSTRUCTURE
SUPPORTING CLAMP AND SEPARATING DEVICE (TYP, 3 PLACES)
INSULATION, DYNA-QUARTZ, MAINLY SiO_2
UNIT EJECTION PATH
INSULATION, MULTIPLE ALUMINUM FOIL
RETAINER FOR INSULATION, RENE 41 OR HAYNES 25
INSULATION, MULTIPLE FOIL
RADIATOR FIN, Be
C
E
GUIDE PLATE, Ti
THERMOPILE, SiGe OR PbTe
LOAD
DEPLOYMENT DEVICE, INCONEL X
RETAINER PLATE, Be
LOAD
℄ RTG UNIT
LOAD
MOUNTING PLATE, STAINLESS STEEL
HEAT SOURCE FUEL CAPSULE (REF)
RETAINER PLATE (REF)
C
E
HEAT SOURCE FUEL CAPSULE, HAYNES 25
RING CLAMP, Ti (3 SECTIONS)
SUPPORTING BRACKET ON MAIN VEHICLE, Ti
SUPPORT BRACKET AND RING CLAMP SEPARATION DEVICE, Ti
MAIN VEHICLE (REF)
UNIT EJECTION PATH
25.0-in RAD (REF)
RTG REENTRY VEHICLE

SECTION A-A

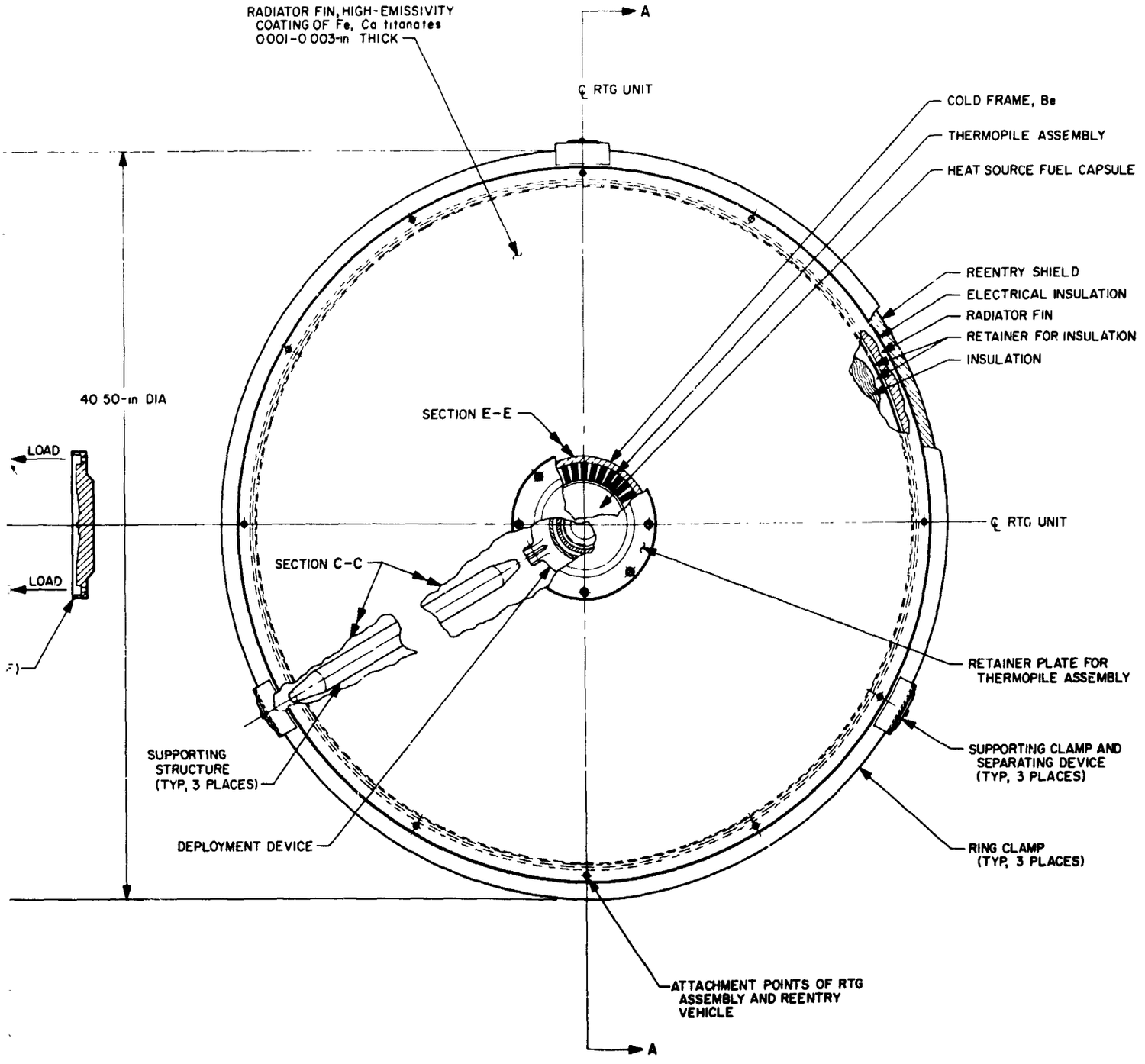

Fig. 1. Radioisotope thermoelectric generator in a reentry vehicle

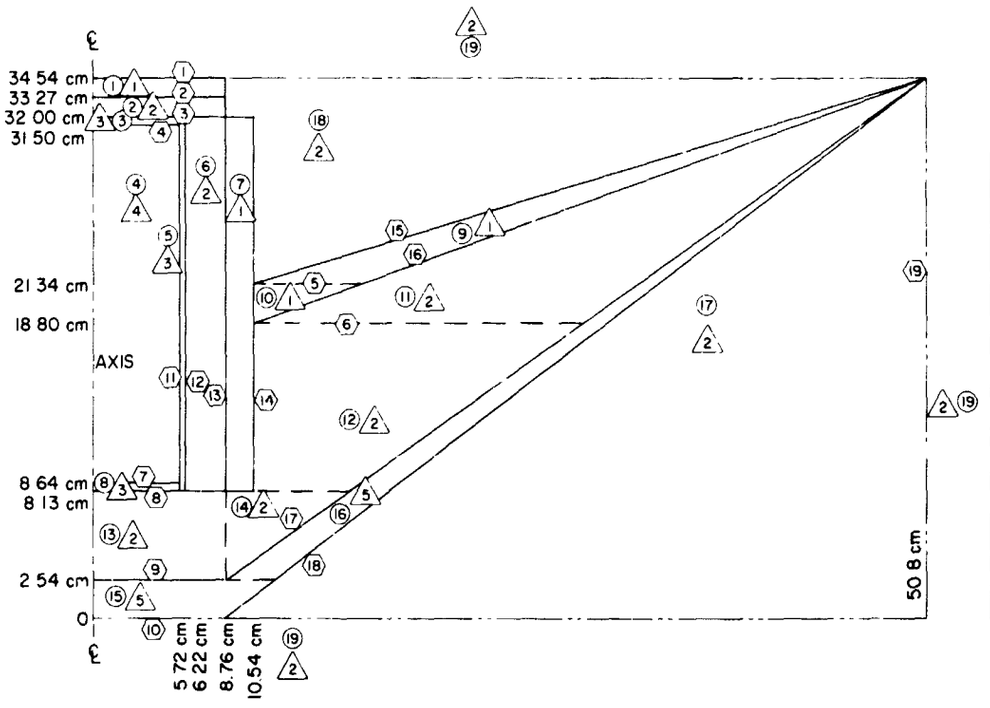

REGION	COMPOSITION	CONCENTRATION, gm/cm³
1	Be	1.84
2	VOID	
3	H-25	9 14
4	FUEL	10 7
5	H-25	9.14
6	VOID	
7	Be	1 84
8	H-25	9 14
9	Be	1.84
10	Be	1 84
11	VOID	
12	2	
13	VOID	
14	VOID	
15	C	1 60
16	C	1 60
17	VOID	
18	VOID	
19	VOID	

Fig. 2. Radiation model of the RTG Headlight configuration

C. Applied Thermionic Research, *O. S. Merrill*

1. Introduction

The results presented here are a summary of work performed between June 1965 and June 1966 under JPL Contract 951262 with Thermo Electron Engineering Corporation (TEECo), Waltham, Massachusetts. This effort is a continuation of a research program which has been in progress for several years. It consists of applied research in thermionic energy conversion and includes both experimental and analytical tasks.

The basic objectives of this effort have been to generate knowledge and to devise techniques for improving the performance of thermionic converters. At the time this contract was initiated, the capabilities of cesium-vapor diodes were well defined, and it was obvious that any step increases in performance could only come from significant changes in the nature of the conversion process. As a result, this program undertook the study of two new regimes of operation.

The first was the use of CsF vapor in addition to metallic cesium in the converter. The presence of CsF causes the Cs vapor to be more tightly bound to the emitter surface, so that the cesium pressure required to maintain a given coverage is greatly reduced. This reduction of Cs pressure results in less scattering of electrons in the plasma, and therefore improved performance. Evidence of these effects had been obtained in the previous year, and an analytical framework forming the basis for further investigation was devised. Questions of stability, however, still remained to be answered before these improvements could be put to effective use.

The second main task of the program was a study of the effects of inert gas additives on the characteristics of the converter. There were three reasons for undertaking this study. Because of the very low cross section of inert gas atoms for low-energy electron collisions, it was hypothesized that inert gases could act as diffusion barriers to Cs ions, thus conserving them, while they remained transparent to electrons. It was reasoned that, if Cs ions were indeed conserved, fewer would be required and the internal voltage loss necessary for ion production in the converter would be reduced. The second reason for undertaking this study was that the presence of an additional gas in the interelectrode space could be used as a tool in the study of the converter plasma. The third reason for this study was the fact that inert gases are major constituents of the fission products of thermionic reactor systems. As such, they may be present in the interelectrode space. It is therefore desirable to know their effects on converter performance.

In the inert gas studies, an etched rhenium emitter was used which, when tested with Cs only, provided a performance reference prior to the introduction of inert gas. It also provided data for comparison with previously-tested rhenium surfaces not electro-etched.

2. Test Converter and Instrumentation

The test converters used in this program are variable parameter research-type devices (Fig. 3). They are of planar geometry and use an active collector guard ring. The parameters whose values can be varied and accurately controlled include the emitter, collector and guard ring temperatures, the interelectrode spacing, the cesium and additive reservoir temperatures and, consequently, the cesium and additive gas pressures.

The emitter is heated by electron bombardment, and its temperature is measured with an optical pyrometer in a black-body cavity located on its back surface. The collector and guard-ring temperatures are maintained by balancing the heat input to their respective heaters against the heat rejected to individual water-cooled coils. The variation of spacing is accomplished by flexing a bellows joining the emitter and collector structures by means of a mechanism operated externally to the belljar. Three micrometer spindles are driven by shafts which are geared together above the top plate. The interelectrode spacing is measured directly on three dial indicators which are set to measure changes in the relative position of the emitter and collector structures.

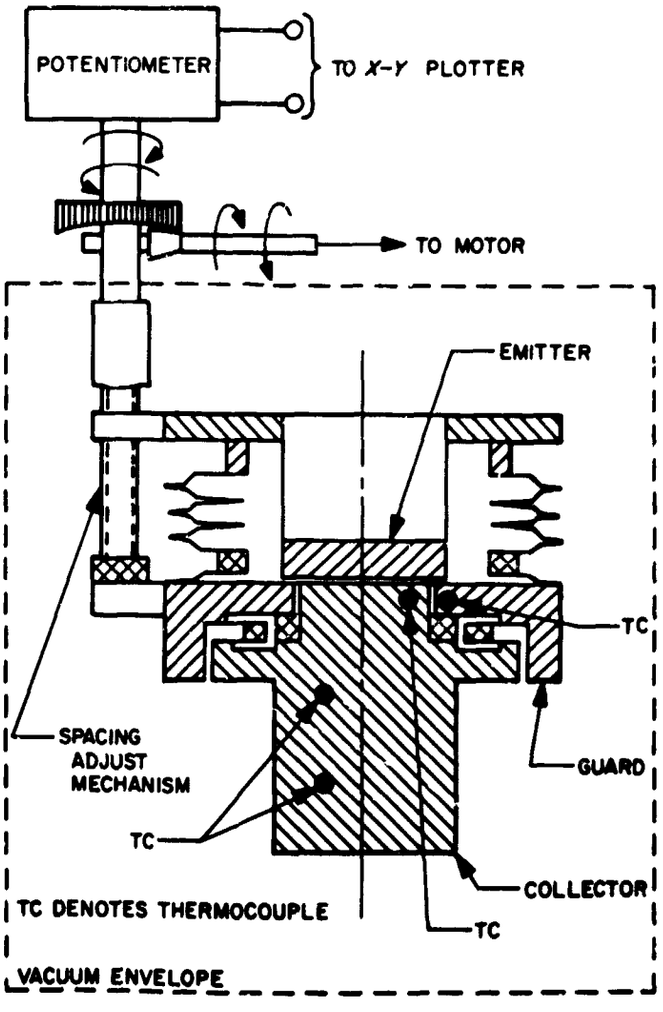

Fig. 3. Schematic of the cesium diode

A tubulation leads from the emitter support structure to the cesium reservoir. A similar reservoir is used for the cesium fluoride. The only difference between the two is that the entrance to the tubulation leading to the cesium reservoir is restricted by a 10-mil orifice. This orifice prevents cesium fluoride vapor from condensing in the cesium reservoir at a rapid rate. In the case of the plasma-additive converter, inert gas is introduced by means of a tubulation leading from the cesium reservoir to the exterior of the vacuum envelope of the converter and to the inert-gas injection system.

3. Experimental Procedure

The two main types of experiments performed under this program were quasi-static, low-power work function and dynamic, high-power performance tests. In each of these, the output was obtained in the form of current density-voltage plots on an x-y recorder. Valid data required that there be no electrode temperature variation during a particular run.

The emitter work function, ϕ_E, was determined from the emitter saturation current, J_S, obtained at a given emitter temperature, T_E, by substituting these values into the Richardson equation,

$$\phi_E = -kT_E \ln J_S/AT_E^2$$

where k is the Boltzmann constant, and A is the Richardson constant. The validity of the results is strongly dependent upon the measurement of the true value of saturation current density. A sufficiently large electron-accelerating voltage must be employed to ensure that the emitter work function is the only barrier controlling the current. Ion-rich temperature conditions must be established to eliminate any space-charge barrier formation. A further requirement introduced by back-scattering of electrons in the plasma is that spacing be held to small values, on the order of 1 mil.

The most useful method of measuring collector work function is the retarding plot. The J-V characteristic for an idealized diode, shown in Fig. 4, is made up of two curves; the first is given by

$$J = J_S \qquad \text{for } V < V_c$$

and the second by:

$$J = AT_E^2 \exp(-\phi_c + V/kT_E) \qquad \text{for } V > V_c$$

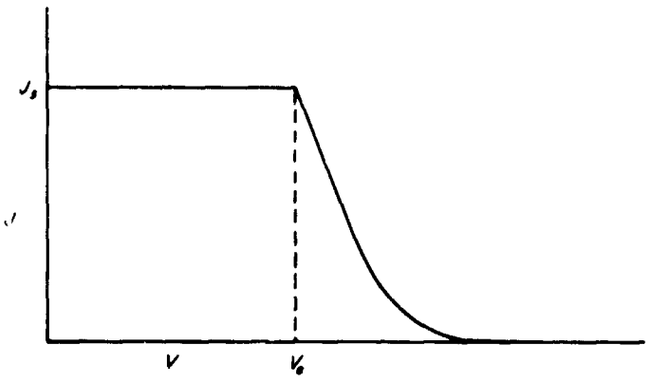

Fig. 4. Ideal J-V diode characteristics

Any point on the exponential part of the characteristic can be used to compute collector work function by substituting J, V and T_E in the second equation. Satisfactory testing with this technique requires low collector temperature (for low back emission), low emitter temperature (for low ion currents), and small spacing (because of scattering effects). The low current levels associated with these measurements allow the use of the quasi-static equipment which, at the same time, provides the accurate guard potential control necessary to eliminate leakage effects.

The high-power performance tests were those wherein "parametric data" or families of current-voltage characteristics are generated through the systematic variation of parameters. Such families may be generated by using as the variable parameter either the emitter temperature, the spacing, the collector temperature, or the cesium reservoir temperature, all other parameters being held constant. In general, the range of variation covered included the region of interest for power production. Therefore the emitter temperature range extends from 1600 to 2050°K, the spacing from 0.2 to 60 mils, and the Cs reservoir temperature from 540 to 700°K. Since this is the high-current region of the characteristics, the dynamic test equipment must be used.

4. Emitter Preparation

The experimental work using cesium fluoride additive was conducted in a tungsten-emitter converter. The inert-gas additive converter used a rhenium emitter.

Two polycrystalline tungsten emitters were prepared with electro-polished and heat-treated surfaces. The changes on the emitter surface which were observed to occur during preparation were grain growth and grain boundary grooving. Each of these changes was expected on the basis of prior experience. Since the emitter is exposed to much lower temperatures during diode operation, and the rate of surface change decreases with time, no further changes were expected to occur during testing.

One polycrystalline rhenium emitter was prepared with an electro-etched and heat-treated surface. Following this preparation, the emitter surface showed rounding and smoothing of the etched surface and faint traces of grain movement as expected on the basis of prior experience. As with the tungsten emitter, the rhenium emitter was expected to be completely stable during diode operation.

5. Additive Studies

a. Cesium fluoride. Under a previous JPL Contract 950671, an impressive diode performance was achieved using CsF as an additive (Fig. 5). However, the improved performance was not stable and after approximately 30 hr the output would revert to a value such as would be obtained without the additive. The first converter tested with CsF exhibited the "additive effects" anticipated but, just as with previous devices, this effect disappeared after 50 hr of testing. A series of diagnostic testing with this device supplemented with glass tube experiments, mass spectrometry and an extensive literature study of related work indicated that water contained in the CsF was responsible for the "additive effects" observed in this work and that reported in the literature (Fig. 6). Furthermore, the literature survey pointed out that almost all past investigations used CsF not sufficiently out-gassed to remove the water. It also became obvious that extreme care must be used in any of these investigations to exclude oxygen, since as little as 10^{-8} torr was sufficient to cause a pronounced work function shift. In normal cesiated converters, these effects are not observed since the cesium quickly "getters" the limited amounts of oxygen present. The significant results obtained from these converter studies may be summarized as follows: (1) There is an apparent threshold in the additive effect; stable effects do not appear until a certain additive reservoir temperature is reached, usually about 700°K. (2) Only two stable work

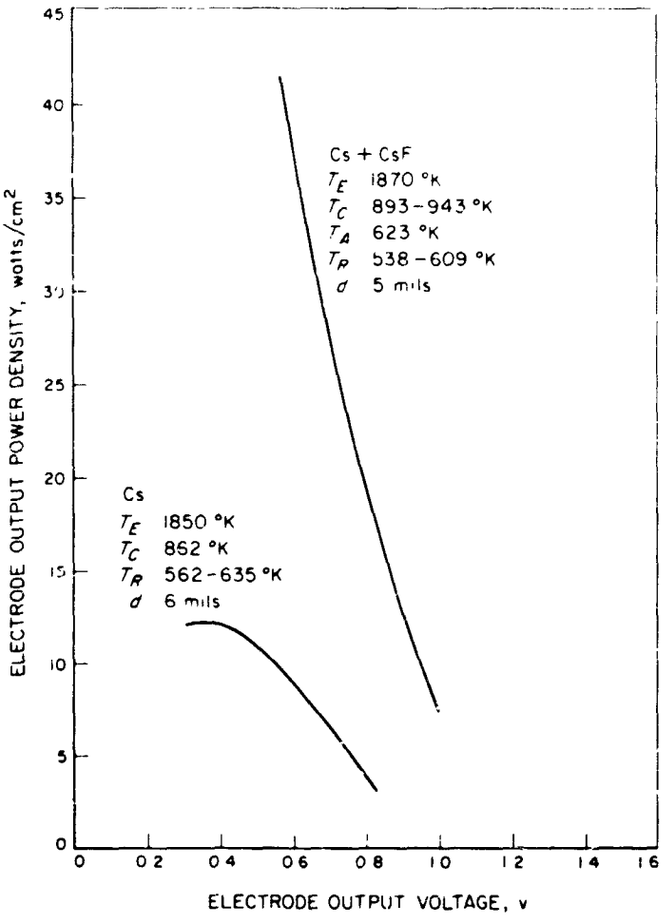

Fig. 5. Comparison of power output with and without additive

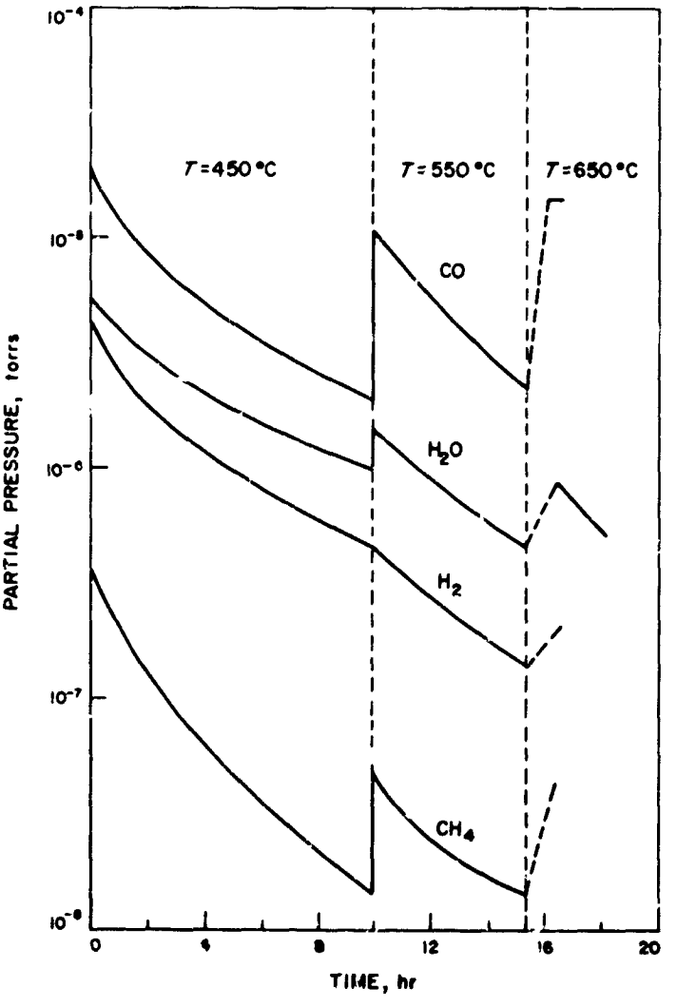

Fig. 6. Mass spectrometer analysis of CsF outgassing

function levels have been observed for tungsten, a bare work function at about 4.8 ev and an "additive" work function at about 5.3 to 5.5 ev. (3) When a high CsF reservoir temperature is used together with a high emitter temperature, the work function values soon decay to the bare level and a permanent degradation occurs. (4) After degradation, CsF is still present in the device with a pressure responsive to its reservoir temperature. (5) After degradation, conditions favoring abnormally high additive coverage, such as low emitter temperature, soaking or raising of collecter temperature, produce a short transient increase in work function. (6) After degradation, very high additive reservoir temperatures do not produce significant changes in work function beyond a short transient.

Two possibilities for the loss of additive effect were proposed: either a contaminating substance had been introduced along with the CsF or else the test vehicle emitter had become "poisoned" and responsive to CsF vapor. It was determined that it was the water contamination contained in the fluoride which was responsible for the observed results

In view of these findings, the surface additive task was divided into two parallel efforts. The first was devoted to the investigation of the effects of pure CsF on the work function of tungsten at thermionic temperatures. The second was devoted to the investigation of the effects of oxygen.

To accomplish the first effort, a special metal-ceramic tube was designed and fabricated (Fig. 7). In this vehicle it was possible to exercise better control of the test vehicle atmosphere in order to isolate and measure the effects of pure CsF on the emitter surface. The new vehicle employed fabrication and testing techniques capable of reducing residual gas pressure to extremely low values,

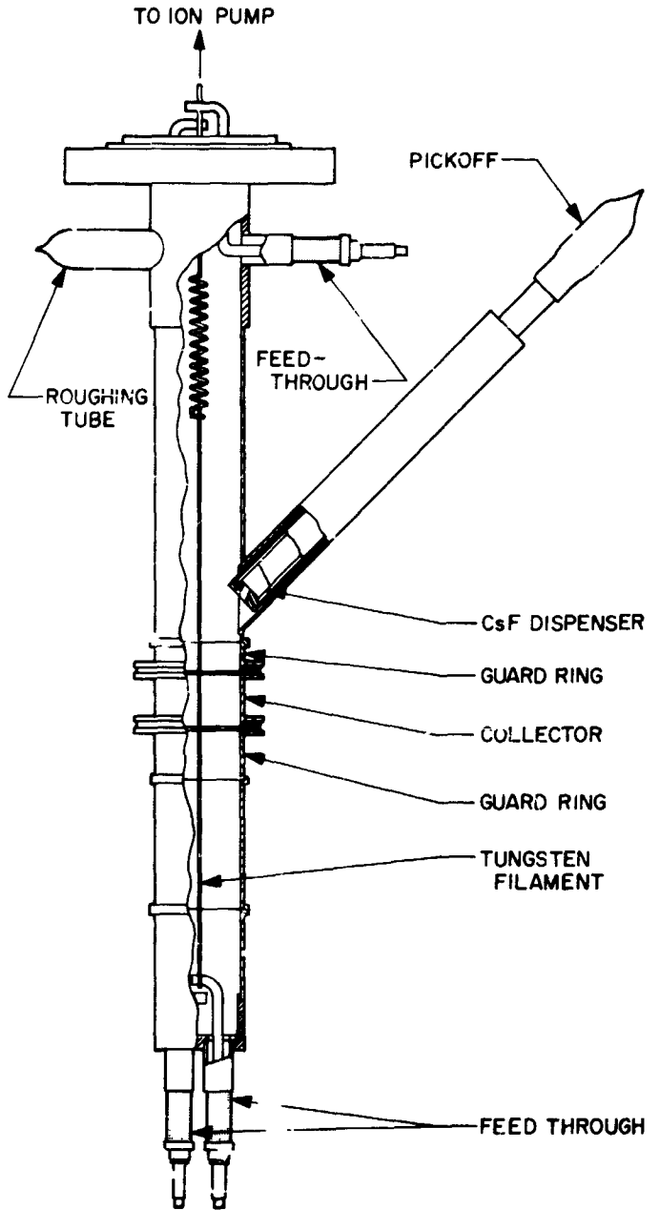

Fig. 7. Surface studies device

i.e., 10^{-11} torr. Results obtained using this device show a maximum increase in work function of the tungsten with CsF additive of 0.3 ev, from 4.6 to 4.9 ev. The arrival rate for cesium ions onto the tungsten filament was 0.3 $\mu a/cm^2$ and was evaluated by measuring the cesium ion current produced by the dissociation of the CsF on the hot filament.

The energy for desorption was derived from the same experiments and was about 3.3 ev. With the relatively small change in work function and the high arrival rates required, it appears that the fluorine additives hold little promise for improving converter performance.

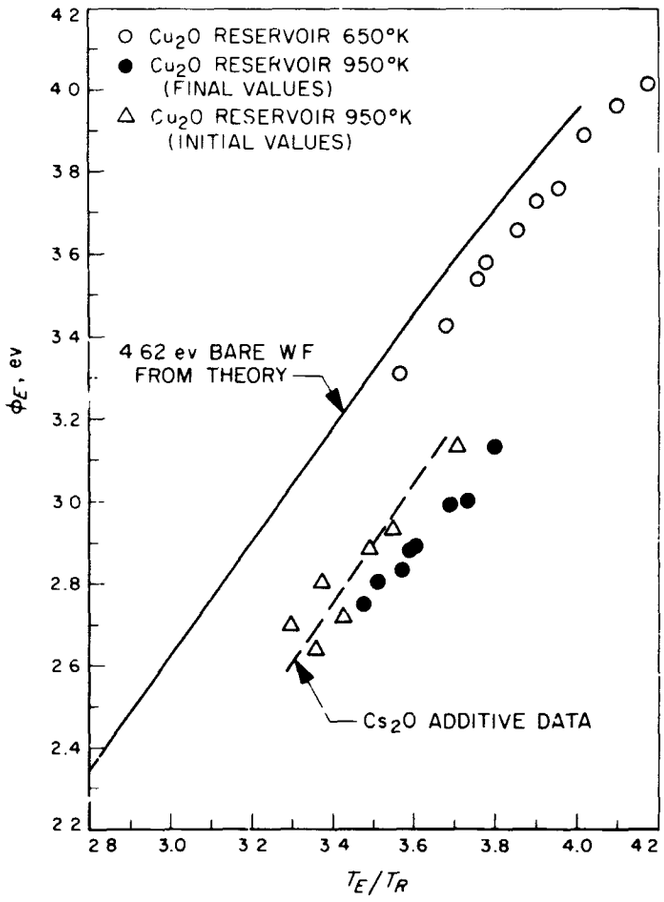

Fig. 8. Tungsten emitter work function comparison

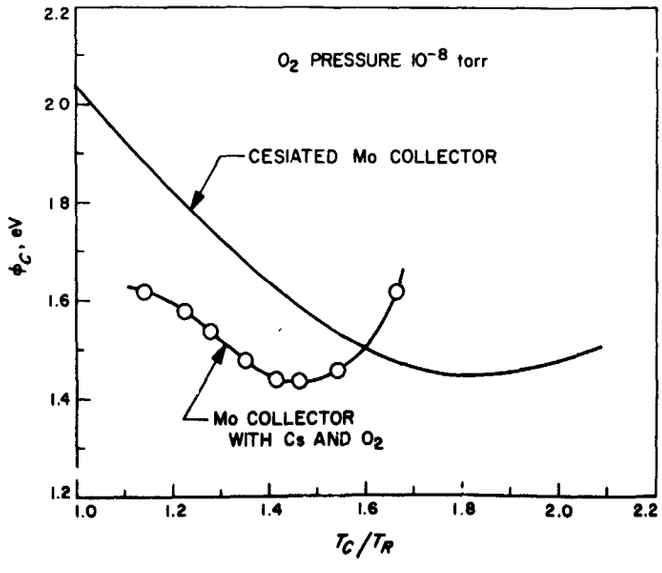

Fig. 9. Cesiated molybdenum collector work function comparison

b. Oxygen. The thermodynamic equilibrium of oxygen in the converter environment was analyzed and the conclusions reached that the oxygen pressure required for coverage was chemically compatible with this environment in the vicinity of the collector. A critical experiment was conducted using Cs_2O as the O_2 source. The emitter work function and power output of the device closely resembled those of the CsF charged devices. This converter was tested for stability for 130 hr without discernable change. A second converter specifically designed for oxygen additive using a Cu_2O oxygen source was tested for 300 hr, producing consistent and reproducible data.

Experimental results indicate that the addition of oxygen to the test converter with a tungsten emitter and a molybdenum collector has resulted in a reduction of approximately 0.45 ev in the emitter work function for the same ratio of emitter to cesium reservoir temperatures (Fig. 8). The effect of the oxygen additive on the collector work function is shown in Fig. 9.

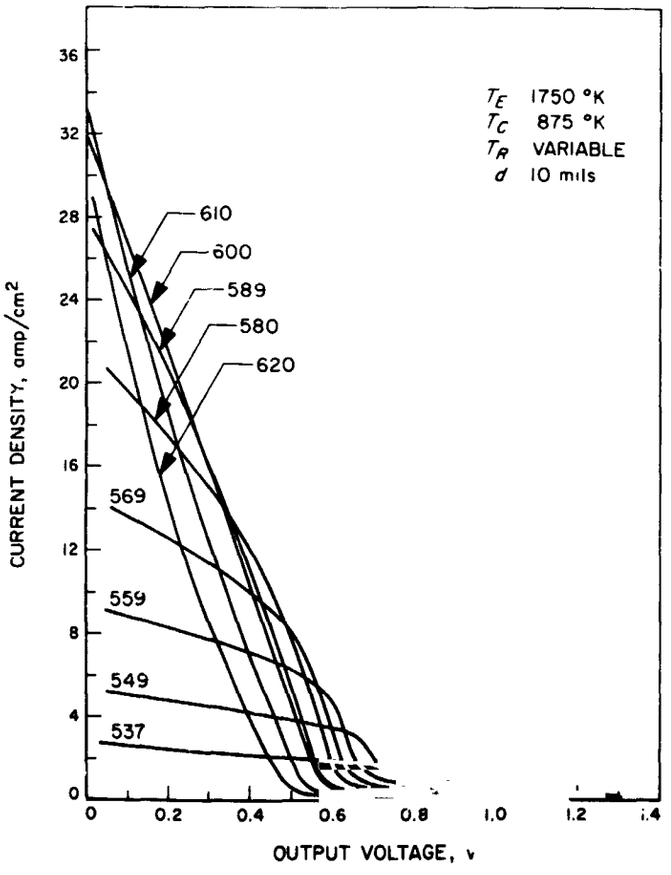

Fig. 10. *J-V* family with cesium only converter; W-emitter, Mo-collector

The results of two mappings of performance parametric data, at similar operating conditions, are shown with cesium only in Fig. 10 and with cesium plus Cu_2O additive in Fig. 11. Both converters have a tungsten emitter and a molybdenum collector. The envelopes of these families are shown together in Fig. 12 for the purpose of comparison. A significant feature of the oxygen converter charac-

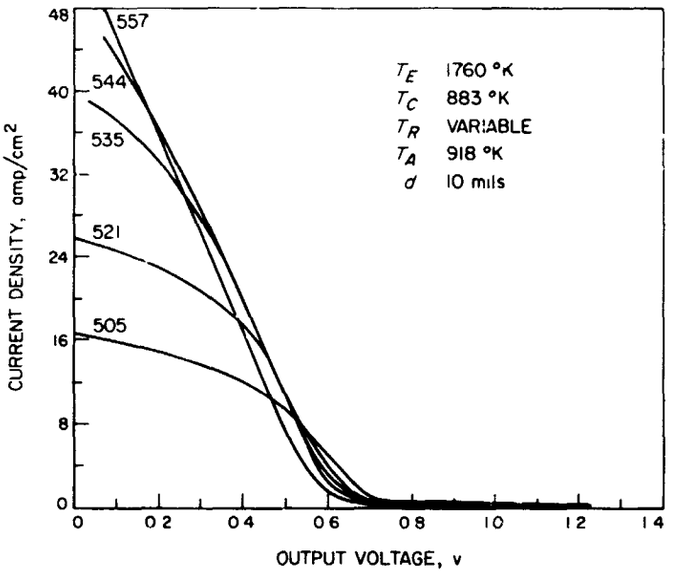

Fig. 11. *J-V* family with cesium—copper oxide converter; W-emitter, Mo-collector

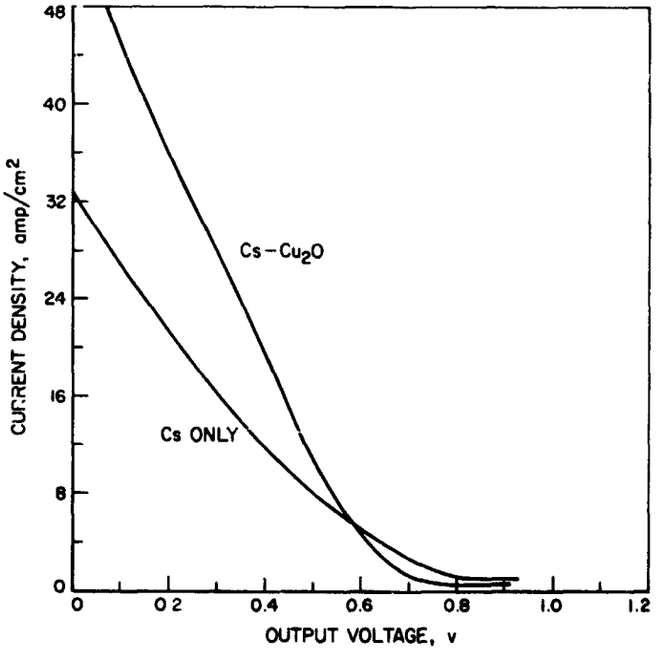

Fig. 12. Comparison of envelopes of *J-V* family curves

teristics when compared to the Cs only data is the steeper slope of the envelope in the oxygen case. The slope change is a direct result of the lowered cesium pressure through the reduction in scattering.

The oxygen additive converter experiments have demonstrated that the enhanced power output first associated with CsF can be maintained through the use of oxygen for at least 300 hr of operation with no degradation. A typical performance curve showing the comparison of power output versus voltage for converters with polycrystalline tungsten emitters and molybdenum collectors for Cs-only versus Cs plus Cu_2O is shown in Fig. 13.

c. Inert gas. The philosophy of the use of an inert gas additive in a thermionic diode may be summarized as follows: electron currents in thermionic diodes are attenuated by two processes, the formation of electron space charge in the interelectrode spacing which results in buildup of potential barriers for electrons, and electron scattering. Electron space charge in cesium diodes can be neutralized by the cesium ions that are produced in the discharge. These ions, however, are short-lived in the interelectrode spacing due to leakage out of the boundaries; they must therefore be continuously generated to maintain a steady density in the plasma. Loss of the ions due to leakage can be reduced appreciably if the diffusivity of the ions is decreased. This can be achieved by addition of a gas to provide scattering centers for the ions. Most of the gases that have a high scattering cross section for cesium ions also attenuate electron current. Inert gases, however, are an exception to this rule. These gases have a high scattering cross section for ions, but at operating electron temperatures their scattering cross section for electrons is very small. Hence addition of an inert gas to the plasma was expected to preserve the ions while leaving electron current virtually unaffected. A comparison between three inert gases, argon, krypton and xenon, revealed that argon would attenuate the ion current and the electron current by significantly smaller amounts than either krypton or xenon as shown in Table 3. Hence, early in the study, argon was chosen as the inert gas to be used in the subsequent experimental investigations.

Table 3. Effect of addition of 1 torr of inert gases in a 10-mil-spacing plasma at 1000°K

Inert gas	Ion current attenuation, %	Electron current attenuation, %
Argon	64	0.7
Krypton	72	1.4
Xenon	78	3.2

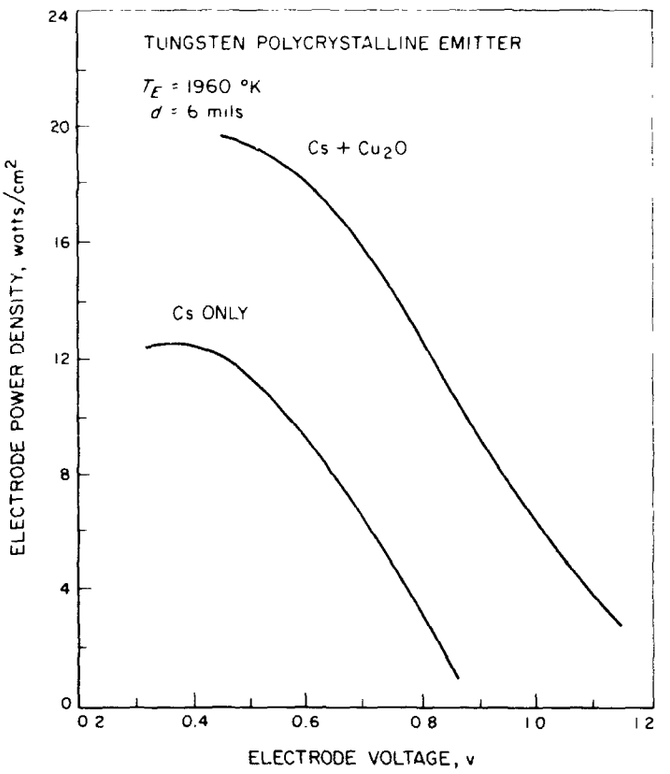

Fig. 13. Power density comparison of converters with Cs only and with Cs plus Cu_2O

The experimental apparatus consists of a variable-parameter diode (previously described) and a gas injection system shown in Fig. 14. The high-purity argon is stored in a cylinder equipped with a two-stage regulator. The gas is introduced into a 75-cc stainless-steel cylinder at a pressure of about two atmospheres. A microflow valve allows the rest of the system to be filled to the desired pressure (in the range of 0.2 to 200 torr). The inert gas passes through a cold trap and a hot zirconium trap to minimize the impurities. The gas pressure in the converter is monitored by a diaphragm pressure gage. The pumping system consists of an ion pump, which can be isolated by an all-metal on-off valve, and a mechanical pump used for roughing the entire system.

Several hundred variable-spacing families of volt-ampere characteristics were obtained. The data covers the cesium temperature range of 533 to 563°K at emitter temperatures of 1675 and 1800°K, and the argon pressure range of 0 to 100 torr. These data conclusively show that there is no enhancement of performance under any conditions in the presence of argon. A gradual decrease in output was observed with increasing inert gas pressure.

However, argon appears to have little effect on the characteristics at pressures below 20 torr. This result is of particular interest to nuclear thermionics, since inert gas fission products may enter the interelectrode space of converters located in a reactor core. Typically, 10 torr of argon would result in a 10% reduction in the output of the converter. Two torr of krypton or one torr of xenon would have the same effect.

6. Rhenium Emitter Preparation

To provide a reference for comparison in the evaluation of the ion conservation capabilities of argon, the performance of an electro-etched rhenium emitter was documented through a parametric mapping using Cs only. The parametric mapping of the etched rhenium emitter revealed that the etching preparation resulted in a two-fold improvement in performance over a polished rhenium emitter. Alternatively, the etched rhenium emitter gives the same performance at twice the spacing required by a polished rhenium emitter. A comparison of the work functions of electroetched and electropolished rhenium is given in Fig. 15.

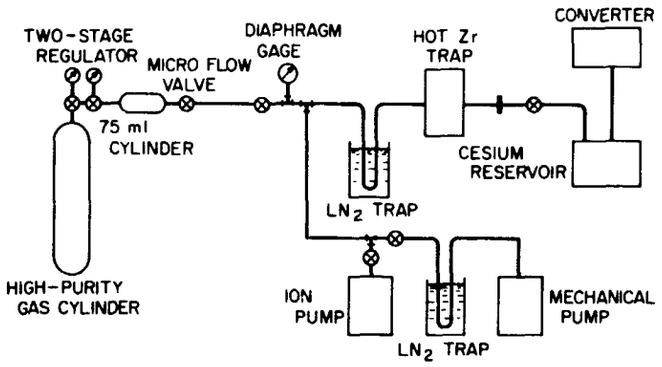

Fig. 14. Inert gas injection system

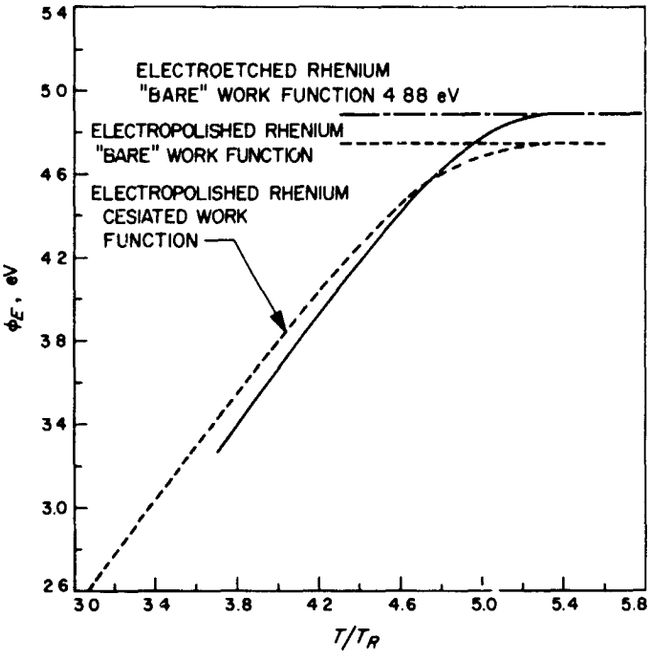

Fig. 15. Comparison of the work functions of electroetched and electropolished rhenium

References

1. Kitrilakis, S., et. al., *Final Report, Thermionic Research Program*, JPL Contract 951262, Report TE 12-67, Thermo Electron Engineering Corp., Waltham, Mass., August 1966.

2. Kitrilakis, S., et. al., *Final Report for the Thermionic Research Program*, Task IV, JPL Contract 950671, Vol. I, Report TE 7-66, Thermo Electron Engineering Corp., Waltham, Mass., August 1965.